NANOSTRUCTURED TiO_2/Ti BASED ELECTRODES OBTAINED FROM TITANIUM SCRAP

Laura Eugenia BARBULESCU [1, 2]

The aim of this paper is to transform a waste material (a scrap resulted from mechanical processing of titanium ingots fabrication) into a useful one. Starting from titanium scrap and using anodization, we generate at the surface an anatase nano-architecture, with photocatalytic properties. Copper doping for anatase architecture was the procedure used to enhance the photocatalytic behavior for the new created electrode. Electrochemical surface investigations and high-resolution electronic scanning microscopes images, were performed to demonstrate the photocatalytic behaviour of this transformed waste.

The new created electrode covered with TiO_2CuNPs was successfully used for phenol degradation up to benzoquinone and hydrochinone (phenol partial degradation compounds).

Keywords: Nanostructured TiO_2, titanium scrap, phenol, photocatalytic behavior

1. Introduction

Titanium and its alloys are very important in many applications such as: aeronautics because of excellent mechanical properties and chemical resistance [1], medical purposes due to very good bio-compatibility and bio-reaction capacity with human tissue and plasma [2] and many other applications like degradation of organic pollutants using titanium dioxide (anatase) formed on its surface [3]. This protective coating of TiO_2, which is non-toxic and environmentally friendly, transforms titanium in an interesting material with different applications such as purification of waste water [4] or polluted air [5] and self-cleaning surfaces [6]. TiO_2 is remarkable for generating electrons at suitable wavelength. These electrons jump from valence band to the conduction band generating holes which are useful oxidants for degradation of environmental pollutants. Titanium scrap has been considered to be an eco-friendly waste with a relatively low cost and a suitable candidate to be transformed in TiO_2 with photocatalytic properties in removing environmental pollutants [7-11].This work used anodization of titanium scrap in order to obtain a nanostructure of TiO_2 surface coating. Titanium dioxide has also the ability to create a large surface which is able to become active and capable to retain different metallic cations in

[1] PhD student, Faculty of Applied Chemistry and Materials Science, University POLITEHNICA of Bucharest, Romania, e-mail: laura.eugenia.barbulescu@gmail.com
[2] Eng., National Research&Development Institute for Non-ferrous and Rare Metals - IMNR, Ilfov, Romania

its own nanostructure. Among various elements used as TiO_2 dopants so far, Cu can replace certain Ti^{4+} ions in substitution sites of TiO_2. Cu doping has also a very important role in reducing recombination rates of photogenerated pairs electrons-holes maintaining an increased number of charge carriers [12-14].

TiO_2 has three common crystalline phases such anatase, rutile and brookite, anatase having the highest photocatalytic activity[15]. In this study, X Ray Diffraction (XRD) analyses were performed to demonstrate the presence of anatase. Copper doping, used to increase photocatalytic effect of TiO_2, transforms the large band gap of TiO_2 from (3.2 -3.4 eV) in a narrow band gap (1.6eV)[16] .

In this work it is described how it was created the nanostructured TiO_2-Ti electrode. The photocatalytic properties of the electrode were demonstrated by electrochemical impedance spectroscopy (EIS) and linear sweep voltammetry (LSV) investigations. The application of the new created electrode was to use it for phenol degradation.

2. Experimental

2.1 Reagents

Ethylene glycol 99% (Alfa Aesar), NH_4F (Sigma Aldrich), HF (Merk), HNO_3 (Sigma Aldrich) were used for anodization. Copper doping was achieved using $CuSO_4$ (Sigma Aldrich), H_2SO_4 (95-97% conc. Merck) and NaOH (Merck). Electrochemical testing was performed using $Na_2SO_4 \cdot 10H_2O$ (Sigma Aldrich) and phenol (Sigma Aldrich). Solutions were prepared using purified water (obtained with a Millipore direct-Q UV3 water purification system).

2.2 Methods

2.2.1 Ti scrap anodization

Small pieces of titanium scrap provided from titanium ingots processing, having 1mm thickness and 20 mm long were modified by anodization in order to obtain a TiO_2 nanostructured surface. The scrap was first cleaned in purified water in an ultrasonic bath for 15 minutes. After that, it was immersed in a solution of HF and HNO_3 for 5 seconds. Freshly obtained samples were fixed in the electrochemical cell as an anodic electrode using a Pt foil as counter electrode. A MATRIX MPS-7163 as electrochemical source was connected to the electrochemical cell. TiO_2 nanostructure was achieved applying a raising voltage from 0 to 40 V, with 2 V /10 s step and then kept it constant 2 h at 40V, at room temperature [17]. We used as electrolyte solution ethylene glycol with 0.5% NH_4F and 2% purified water. After anodization, the obtained samples were rinsed with distilled water. At the end, samples were annealed at 450° C for 2 h for a better sample crystallinity.

2.2.2 Copper doping

Copper doping was realized into a three electrodes electrochemical cell, using anodized and annealed Ti scrap as working electrode, a Pt (Metrohm) counter electrode and Ag/AgCl, 3 M KCl, (Metrohm) as reference electrode. Electrodes were immersed in 1mM $CuSO_4$ solution. SO_4^{2-} anions concentration has been set to 10^{-1} M with H_2SO_4 solution to ensure a high conductivity during the reduction process and the pH was adjusted to 3 with NaOH solution. Copper doping was realized by applying reduction potential pulses of -0.4V related to OCP (Opened Circuit Potential) on the working electrode (60 reduction potential pulses of 200ms) [18] .

The reduction potential of -0.4V has been chosen after a single cyclic voltammogram (sweep rate =20mV/s). During the reduction sweep to a negative potential, an increase in the cathode current begins at -0.3V with a visible maximum around -0.4V which can be associated with the reduction of Cu^{2+} ions to metallic Cu on the titanium scrap NTs surface. During the pulsed electrode deposition process a first pulse of -1.0V is applying during 200ms. Then a 60 repetitive sequence of modulated potential is applied. A reduction potential of -0.4V is applied during 200ms immediately followed by a +0.05V pulse (stripping potential) of 50ms. The first pulse was applied to induced nucleation of Cu nanoparticles into scrap NTs surface. The stripping potential was used to fix Cu nanoparticle size while -0.4V potential was used to slowly growing Cu nanoparticles.

2.2.3. ICP-OES investigation

To prove Cu containing in titanium scrap sample (after electrochemical Cu doping and all electrochemical tests were done) it was used ICP-OES Agilent Technologies 725 equipment.

2.2.4. XRD analyses

DRX analyses were performed on BRUKER D8 ADVANCE using DIFFRACplus XRD Commender (Bruker AXS) software to detect TiO_2 polymorphs phases.

2.2.5 Phenol degradation

The modified electrodes were used for phenol degradation. Experiments were carried out using the same Autolab 302N and the same three electrodes cell. The measurements were performed in the potential range: 0 – 1.4V, with a 2.4mV step and 10mV/s scan rate. Electrolyte solution was 10 mM phenol in Na_2SO_4 0.5 M. Eight LSV repetitive measurements were performed to describe the transformation that took place.

3. Results and discussion.

3.1 Surface modification

Fig. 1 illustrates the recorded current *versus* time curve during titanium scrap anodization procedure. As it is shown in Fig. 1, the curve has three

distinctive areas. The first one corresponds to a strong titanium scrap oxidation phenomenon and as a result, a compact oxide layer is formed on the scrap surface. The red marked area corresponds to the formation of pits in oxide layer while the last one area corresponds to the generation of TiO_2 nanotubes on titanium scrap.

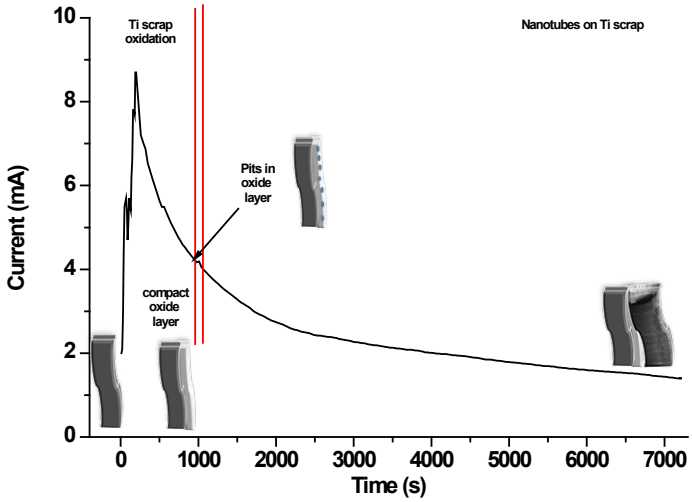

Fig. 1 Current vs. time curve for titanium scrap anodization.

The charge obtained integrating the area under current time curve was 18.83 C.

3.2 SEM images for anodized titanium scrap

SEM images with various magnifications presented in Fig. 2a-d, clearly shows a large area of TiO_2 nanotubes formed on anodized titanium scrap. It can be seen (Fig. 2a-top view image) that TiO_2 nanotubes distribution is uniform. The TiO_2 nanotubes which are opened and cap ended have diameters between 131.3nm and 137.9nm (Fig. 2c).This is a suitable architecture for a highly efficient photocatalyst that minimizes the recombination of photogenerated-electron-hole pairs[19].

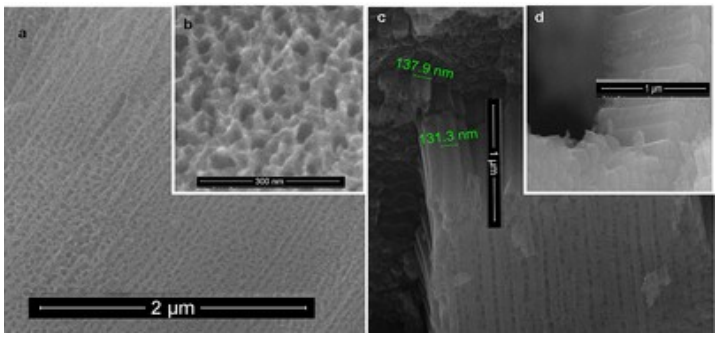

Fig. 2 SEM images for annealed and anodized titanium scrap samples at different magnifications: a,b- top view of nanotubes, c- images of nanotubes (for diameter and high dimension details), d- image of nanotubes presenting cap end

3.3 Copper doping

The Cu deposit during potential modulation is presented in Fig. 3:

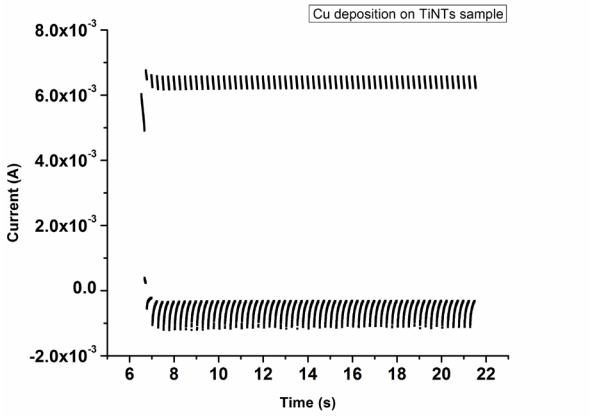

Fig. 3 Plotting for pulsed copper deposition on Ti-TiNTs electrode

Fig. 3 represents the current intensity corresponding to first the first pulse at 1V potential which induce nucleation of Cu nanoparticles (CuNPs) onto titanium scrap NT surface. The positive potential of +0.05V was used to fix the CuNPs size while the potential of -0.4V was used to slowly grow CuNPs resulting in this way rich Cu deposit. In Fig. 4 it is presented the modulation potential method used for Cu deposition. It consists in a 60 repetitive sequences of 15 seconds between -0.4V (the deposition potential) and +0.05V and this potential modulation corresponds to the current intensities recorded from Fig. 3.

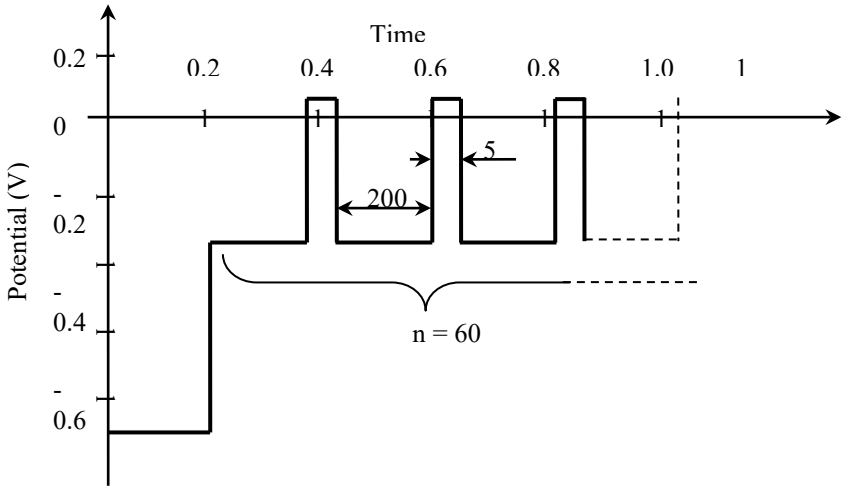

Fig.4. Schematic representation of modulation potential applied for copper deposition

The SEM images presented in Fig. 5 correspond to TiNTsCuNPs samples obtained. The light area observed in SEM images presented in Fig. 5 a-b is due to the copper nanoparticles. SEM images presented in Fig. 5c show the transformation of nanotubes in lamellar nano-walls structure with the thickness of cca 5 μm.

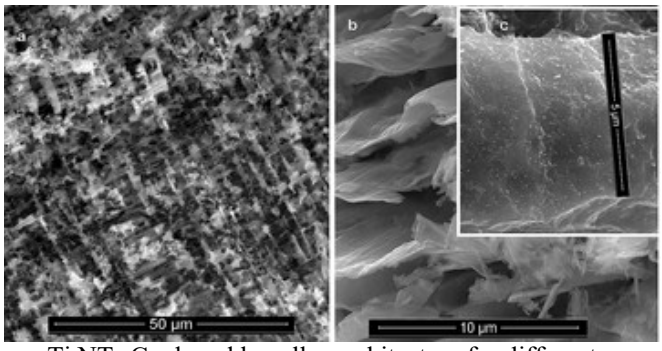

Fig. 5 SEM images Ti NTs Cu doped lamellar architecture for different magnification grades (a,b,c)

Fig. 6 shows details of the inside of new wall structure and new large light area that we assumed to be copper nanoparticles deposits. Copper presence was demonstrated using ICP–OES technique.

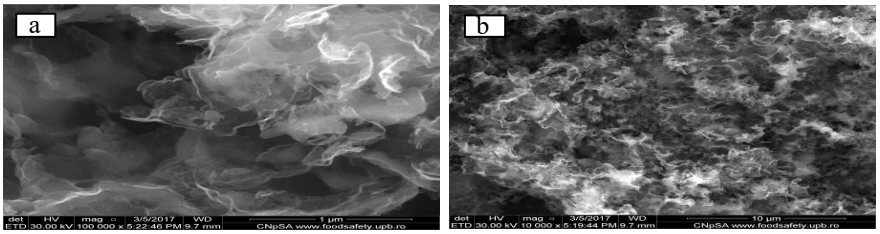

Fig. 6 SEM images for copper deposit in TiNTs samples.(Fig. 5a is for a higher magnification grade than Fig. 5b.)

3.4 ICP-OES investigation

The spectrometric image (Fig.7) for solubilized Ti-TiNTsCuNPs sample shows a clear peak for Cu at 324.75 nm meaning that new created electrode contains copper. The analytical result using ICP-OES technique for this sample was 0.0038% Cu for entire titanium scrap sample. Analyzed sample weight was 0.4473g.

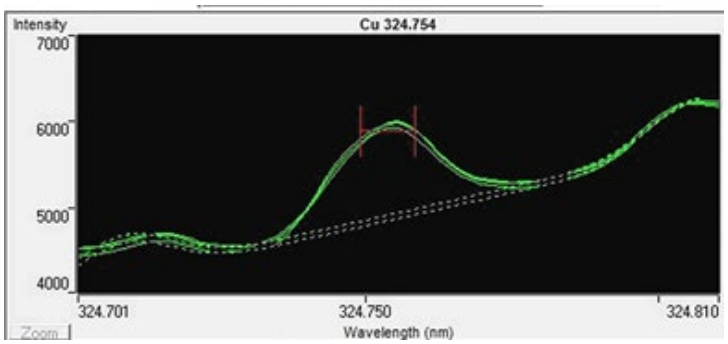

Fig. 7 ICP-OES spectra for titanium scrap copper doped solubilized sample

3.5 XRD analyses

Fig. 8 presents XRD patterns of anodized and annealed titanium scrap sample; it can be observed a small peak at 2θ=25.3° that indicates anatase presence. XRD peaks at 2θ=38° with high intensities are attributed to titanium – which is the substrate for the nanostructured coating. It was expected a low amount of anatase because titanium transformation took place only at sample surface. No other TiO_2 polymorphs such as rutile or brookite were detected by XRD. The annealing sample is considered responsible for the formation of this phase (anatase).

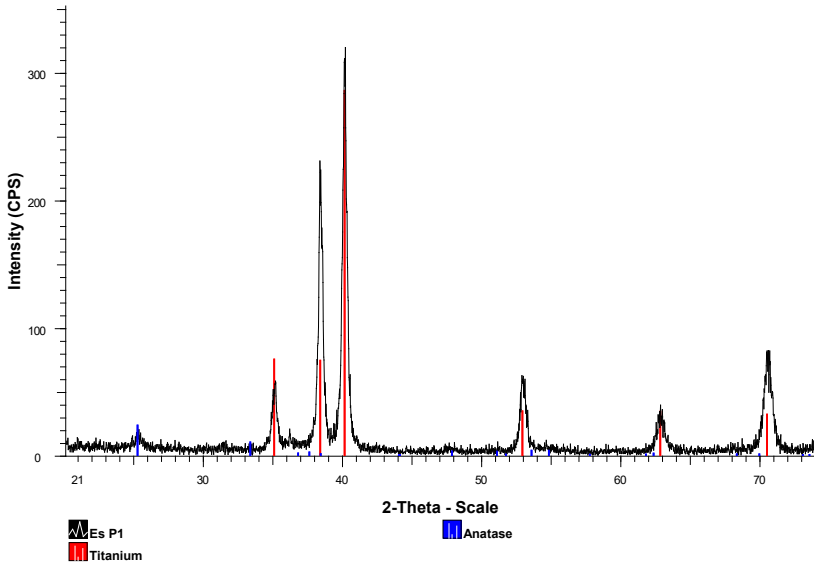

Fig. 8.XRD patterns for anodized and annealed titanium scrap sample.

3.6 Surface electrochemical investigations

To demonstrate the surface activation of the TiNTsCuNPs obtained sample, EIS and LSV tests were performed. Fig. 9 presents Bode phase diagram. In this plotting it can be observed modulus linear variation for the both sample

(TiNTs and TiNTsCuNPs) on the intermediate and low frequency ranges with a negative slope. This is a characteristic of capacitive behavior. The impedance curve for TiNTsCuNPs sample is shifted to lower values than TiNTs sample impedance plot which means a better electronic conductivity for this sample. Maximum angle phase value is -50° for TiNTs sample and it is reduced to -35° for TiNTsCuNPs sample as it can be seen in Fig. 9. Ideal capacitive behavior reaches the phase angle value of -90°. Normally TiO_2 phase angle has values between -65°and -75°. In this case the phase angle decreases is due to titanium sample support, the new nanoarchitecture built being a thin layer on titanium scrap surface. Even there is not an important impedance drop for TiNTsCuNPS sample compared to TiNTs sample impedance, the photocatalytic properties for the new created electrode were enhanced.

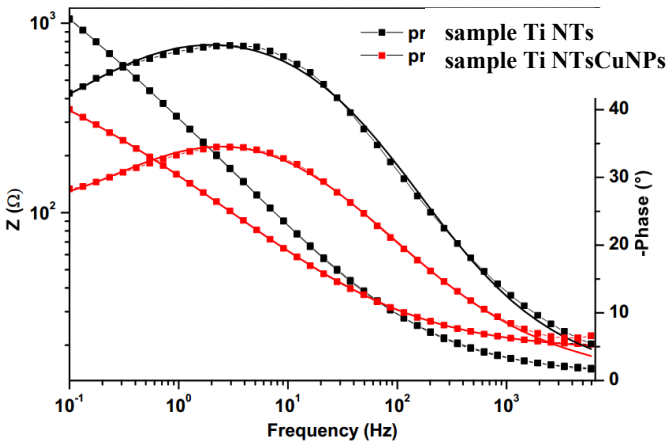

Fig. 9 Bode phase diagram for TiNTs and TiNTsCuNPs samples.

From Nyquiest diagram presented in Fig. 10, one can conclude that TiNTsCuNPs sample presents lower impedance than TiNTs sample meaning a better conductivity. This is in perfectly agreement to the higher current intensity found for the same sample which is presented in Fig. 13 (current – voltage diagram). It can be noticed that there is not a significant difference regarding the impedance for TiNTsCuNPs sample under light or dark conditions, but their impedance values are maintained low (Fig. 11).

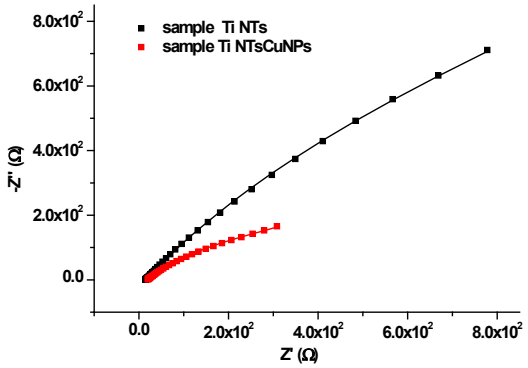

Fig. 10. Nyquist diagram for TiNTs and TiNTs CuNPs samples

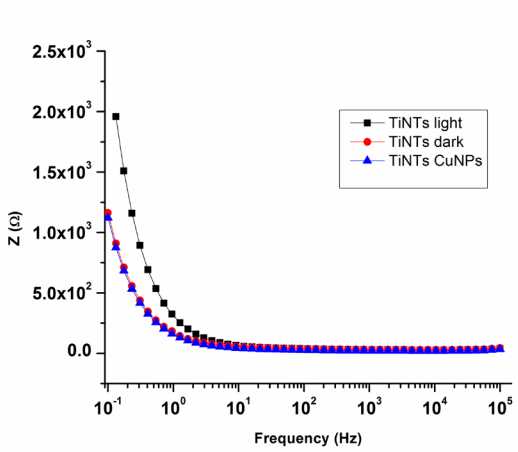

Fig. 11. EIS plotting for TiNTs in dark and light conditions and TiNTs CuNPs samples.

From electrochemical impedance spectroscopy investigation, Fig. 11, it can be seen a decrease for TiNTsCuO electrical resistance; this explains the samples photocatalytic behaviour which is in a good agreement with Nyquist plotting and electrical equivalent parameters calculated and presented in Table 1 and Fig. 12.

Table 1

Parameters for electrical equivalent circuit

Sample	$R_s(\Omega)$	$R_{NT}(\Omega)$	$CPE_{NT}(F)$		R_{OCL} (Ω)	$CPE_{OCL}(F)$		χ^2
			$Y_0(S\cdot s^n)$	n		$Y_0(S\cdot s^n)$	n	
Sample TiNTs	14.221	2.893* 10^3	9.814* 10^{-4}	0.620	8.447* 10^3	18.894* 10^{-4}	0.624	6.241* 10^{-3}
Sample TiNTsCuNPs	18.696	**0.547* 10^3**	21.61* 10^{-4}	0.532	8.617* 10^3	88.289* 10^{-4}	0.523	6.61* 10^{-3}

EIS data were fitted with Nova 1.7 software and it was established the most suitable electrical equivalent circuit for the both mentioned samples, circuit which is presented in Fig. 12.

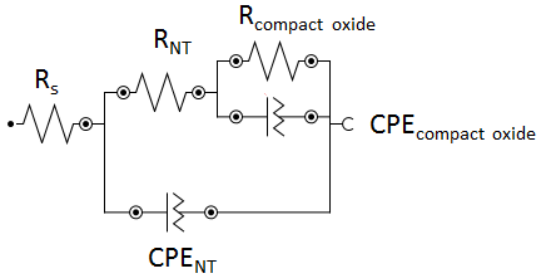

Fig. 12. Electrical equivalent circuit for TiNTs and TiNTsCuNPs samples.

In Table 1 and Fig. 12, Rs represent solution resistance, R_{NT} means nanotubes resistance, $R_{compact\ oxide}$ is the resistance of the compact oxide layer, $CPE_{compact\ oxide}$ is the pseudo-capacitance for compact oxide layer and CPE_{NT} is the pseudo-capacitance for nanotubes layer.

It could be seen in Nyquist diagram (Fig. 10) that the resistance for sample with TiNTsCuNPs decreases in a satisfactory way. The resistance for nanotubes R_{NT} also decreases from $2.893*10^3$ Ω in TiNTs sample to $\mathbf{0.547*10^3}$ Ω in TiNTsCuNPs sample meaning a higher current passing through the sample, the oxide layer becoming more conductive and qualifying the new electrode for photocatalytic phenol degradation.

To demonstrate the new electrode photocatalytic performance, it was built a plot of current vs. potential. From the voltammogram presented in Fig.13, it is noticeable the high current intensity for the TiNTsCuO sample relative to the Ti scrap and TiNTs samples intensity, which explains the new created electrode photocatalytic properties. Current intensities for TiNTs and TiNTsCuNPs sample are very similar, actually they are superposed and difficult to be observed in Fig. 13.

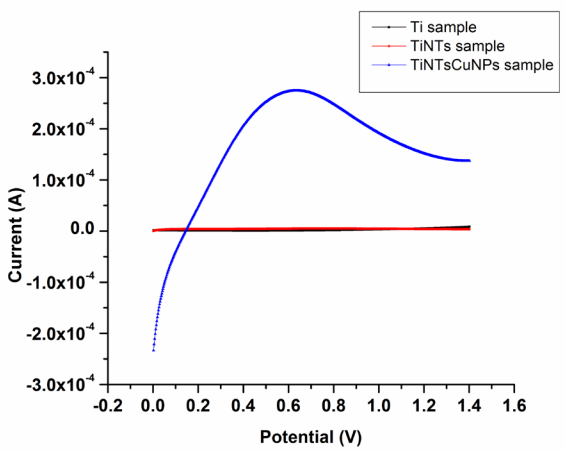

Fig. 13 Voltammogram for Ti scrap, Ti NTs sample and TiNTsCuO sample

Mott Schottky investigation is presented in Fig. 14 and Table 2 lists the flat bad potentials (F_b) and carriers densities (N_d) for TiNTs and TiNTsCuNPs samples in light conditions. From Table 2, flat band potentials are quite close as values while in the case of TiNTsCuNPs sample the value obtained is slightly negatively lower as it was expected. Scientific literature shows that copper doping concentration for TiO_2 increases the F_b values becomes more negatively up to -0,55V [20]. Carrier density is higher for TiNTsCuNPs than for TiNTs sample meaning an electrochemical activation which sustains the sample photocatalytic behaviour.

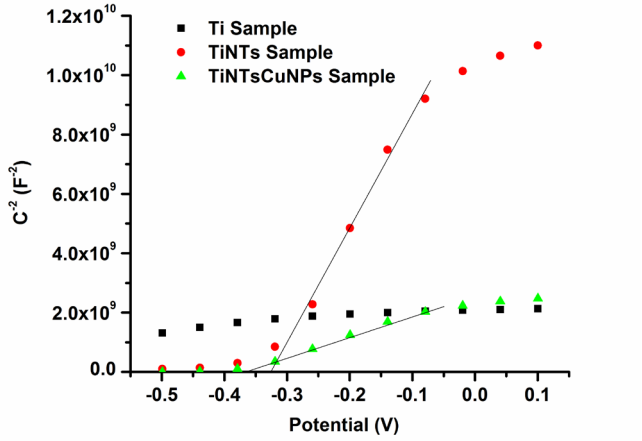

Fig. 14 Mott Schottky investigation

Table2

Flat band potential (Fb) and carrier density values (Nd) for lighted TiNTs and TiNTsCuO samples.

Fb(V)	Nd(cm^{-3})	Sample
-0.334	$3.85 \cdot 10^{17}$	TiNTs light
-0.370	$1.97 \cdot 10^{18}$	TiNTsCuO light

3.7 Phenol degradation

Modified electrodes were used for phenol degradation. LSV investigations were performed for TiNTsCuO sample with phenol solution in order to demonstrate the pollutant degradation. The test realized consists of eight measurements starting from initial moment until to 38 minutes in the same conditions treatment. LSV plotting are presented in Fig. 15.

The experiment was focused on the variation of the current intensity in order to explain the electrochemical processes carried out. Due to the sample with anatase coating that has photocatalytic properties, the created holes generate reactive hydroxyl groups that attack the aromatics nucleus of phenol resulting benzoquinone and hydroquinone. If sufficient hydroxyl radicals are generated, the process is carried out up to maleic acid or oxalic acid and, finally to CO_2 and H_2O. In our case the degradation process takes places only up to form benzoquinone and hydrochinone. Cyclic voltammetry studies present a peak potential for benzoquinone at 0.1V and for hydrochinone at 0.5V, these potentials strongly depending on the electrolyte added [21].

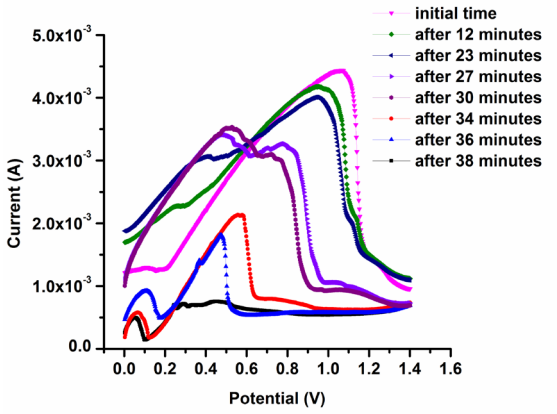

Fig. 15 Linear sweep voltammetry for TiNTsCuNPs as electrode immersed in an electrolyte of Na_2SO_4 enriched with phenol

In Fig. 15, which is a plot current (A) *vs*. potential (V) repeated at different moments is revealed a large peak around 0.9-1V corresponding to the phenol content which is in perfectly agreement to the scientific literature data [22]. It is

very clear that in time two new peaks will appear, one at 0.5V corresponding to hydroquinone and another one at 0-0.2V due to the benzoquinone obtained. Both benzoquinone and hydroquinone are intermediate compounds of phenol degradation. The reaction mechanism is presented in Scheme 1.

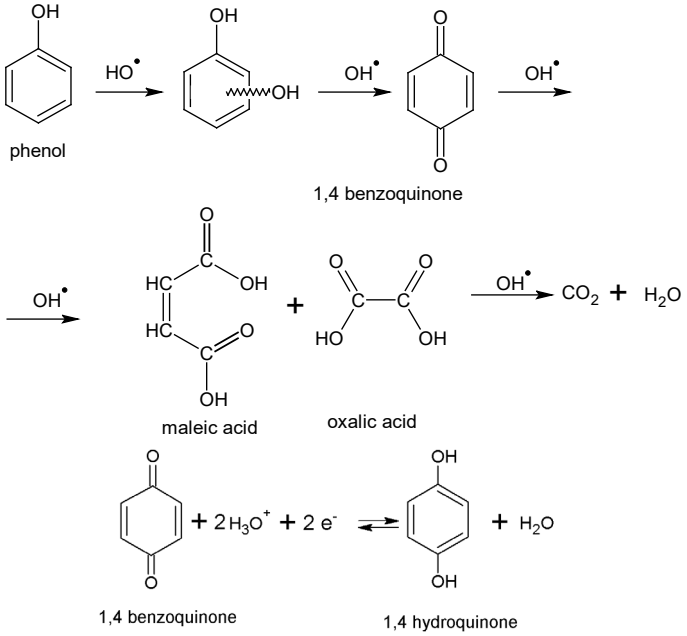

Scheme 1 Phenol oxidation reactions/degradation mechanism

It is clear that, the oxidation process is not a totally one up to final oxidation compounds as it was expected. The explanation could be the irregular shape of the sample and also its roughness that play an important role in nano-structure growing. Both features cannot be perfectly uniform and controlled for the studied samples.

4. Conclusions

The main conclusions of this study are:

- A new electrode was obtained using anodization starting from titanium scrap (unrecycled fabrication sort) provided from a titanium ingots factory in order to obtain a nanostructure of anatase coating on its surface.
- Cooper doping used for anatase nanostructure coating enhances material photocatlytic properties in order to support phenol partial degradation, giving the chance for a waste to become a photocatalytic material.
- The nano-architecture of new created electrode from titanium scrap was put in evidence by SEM images. Due to the photocatalytic behavior, one possible application of this electrode is in phenol partial degradation.

REFERENCES

[1]. Boyer, R.R., An overview on the use of titanium in the aerospace industry. Materials Science and Engineering: A, 1996. **213**(1): p. 103-114.
[2]. de Viteri, V.S. and E. Fuentes, Titanium and Titanium Alloys as Biomaterials. 2013.
[3]. Verbruggen, S.W., TiO2 photocatalysis for the degradation of pollutants in gas phase: From morphological design to plasmonic enhancement. Journal of Photochemistry and Photobiology C: Photochemistry Reviews, 2015. **24**: p. 64-82.
[4]. Zeb, M.A., et al., Effect of waste water treated with TiO2 nanoparticles on early seedling growth of Zea mays L. Journal of Water Reuse and Desalination, 2018. **8**(3): p. 424-431.
[5]. Binas, V., et al., Modified TiO2 based photocatalysts for improved air and health quality. Journal of Materiomics, 2017. **3**(1): p. 3-16.
[6]. Won, Y., K. Schwartzenberg, and K.A. Gray, TiO2-based transparent coatings create self-cleaning surfaces. Chemosphere, 2018. **208**: p. 899-906.
[7]. Methylene Blue and Phenol Photocatalytic Degradation on Nanoparticles of Anatase TiO₂. Polish Journal of Environmental Studies, 2010. **19**(4): p. 685-691.
[8]. Cong, Y., et al., Synthesis of α-Fe2O3/TiO2 nanotube arrays for photoelectro-Fenton degradation of phenol. Chemical Engineering Journal, 2012. **191**: p. 356-363.
[9]. Mahlambi, M.M., C.J. Ngila, and B.B. Mamba, Recent Developments in Environmental Photocatalytic Degradation of Organic Pollutants: The Case of Titanium Dioxide Nanoparticles—A Review. Journal of Nanomaterials, 2015. **2015**: p. 790173.
[10]. Santhosh, C., et al., Photocatalytic degradation of toxic aquatic pollutants by novel magnetic 3D-TiO2@HPGA nanocomposite. Sci Rep, 2018. **8**(1): p. 15531.
[11]. Tsang, C.H.A., et al., Titanium oxide based photocatalytic materials development and their role of in the air pollutants degradation: Overview and forecast. Environ Int, 2019. **125**: p. 200-228.
[12]. Mathew, S., et al., Cu-Doped TiO2: Visible Light Assisted Photocatalytic Antimicrobial Activity. 2018. **8**(11): p. 2067.
[13]. Ganesh, I., et al., Preparation and characterization of Cu-doped TiO2 materials for electrochemical, photoelectrochemical, and photocatalytic applications. Applied Surface Science, 2014. **293**: p. 229-247.
[14]. Bensouici, F., et al., Optical, structural and photocatalysis properties of Cu-doped TiO2 thin films. Applied Surface Science, 2017. **395**: p. 110-116.
[15]. Luttrell, T., et al., Why is anatase a better photocatalyst than rutile?--Model studies on epitaxial TiO2 films. Sci Rep, 2014. **4**: p. 4043.
[16]. Aguilar, T., et al., A route for the synthesis of Cu-doped TiO2 nanoparticles with a very low band gap. Chemical Physics Letters, 2013. **571**: p. 49-53.
[17]. Dumitriu, C., et al., Antibacterial efficiencies of TiO2nanostructured layers prepared inorganic viscous electrolytes. Applied Surface Science, 2015. **341**: p. 157–165.
[18]. Rosenbaum, J., et al., Antibacterial properties of nanostructured Cu-TiO2 surfaces for dental implants. Biomater Sci, 2017. **5**(3): p. 455-462.
[19]. Sreekantan, S., R. Hazan, and Z. Lockman, Photoactivity of Anatase-Rutile TiO2 Nanotubes Formed by Anodization Method. Thin Solid Films, 2009. **518**: p. 16-21.
[20]. Wijayarathna, T.R., et al., A high efficiency indoline-sensitized solar cell based on a nanocrystalline TiO(2) surface doped with copper. Nanotechnology, 2008. **19**(48): p. 485703.
[21]. Quan, M., et al., Voltammetry of Quinones in Unbuffered Aqueous Solution: Reassessing the Roles of Proton Transfer and Hydrogen Bonding in the Aqueous Electrochemistry of Quinones. Journal of the American Chemical Society, 2007. **129**(42): p. 12847-12856.
[22]. Uskova, I.K. and O.N. Bulgakova, Cyclic voltammetry of phenol. Journal of Analytical Chemistry, 2014. **69**(6): p. 542-547.